Swelling and Rheological Characterization of Preformed Particle Gels for Improved Water Shutoff Performance in Core Flooding Tests

Mohammed Khairy M. Salih
Department of Petroleum Engineering, University of Zakho, Kurdistan Region, Iraq
mohammed.sailh@uoz.edu.krd (corresponding author)

Abbas Khaksar Manshad
Department of Petroleum Engineering, Abadan Faculty of Petroleum Engineering, Petroleum University of Technology (PUT), Abadan, Iran
akmanshad113@gmail.com

Sherwan M. Simo
Department of Petroleum Engineering, University of Zakho, Kurdistan Region, Iraq | Engineering Researcher Center, University of Zakho, Kurdistan Region, Iraq
Sherwan.simo@uoz.edu.krd

Received: 12 August 2025 | Revised: 28 August 2025 | Accepted: 7 September 2025

 DOI: https://doi.org/10.48084/etasr.14018

ABSTRACT

There are numerous challenges in producing water effluents in established reservoirs, which could eventually result in their abandonment. Preformed Particle Gel (PPG) is employed in gel to water the cutoff treatment of such reservoirs, a procedure that blocks the channels of fracture and insulates the highly permeable areas. The specific method results in successful conformity control in addition to lowering the water output. In this study, a novel form of PPG with a very high swelling ratio of 250 grams of water absorbed per gram of dry gel (g/g) was introduced. The formulation consisted of acrylamide as polymer, N, N'-methylenebisacrylamide (MBA) as crosslinker, Potassium Persulfate (KPS) as initiator, along with the synthesis of SiO_2/Xanthan Nanocomposites (NCs) and the synthesis of corn oil surfactant (sodium ethyl ester sulfonate anionic surfactant), which together formed the PPG. The PPG functions as a superabsorbent, absorbing water up to 100–250 times the dry weight of the gel. The study examined the effects of the temperature, salinity, concentrations of polymers, cross-linker, and initiator on PPG swelling. According to the results, the PPG swelling ratio decreased as the concentrations of polymers, crosslinkers, and initiator increased along with the salinity. The PPG swelling ratio significantly reduced to within 1000 ppm of SiO_2/Xanthan NCs, with values dropping by nearly 50%. However, the reduction was not significant outside this concentration range, which was referred to as PPG10. For the rheology test, samples of PPG 10 with a 2.5 cP viscosity were selected. The viscosity value of the samples remained consistent for different rotational speeds (60%, 100% and 120%). The blocking effectiveness and performance of the three samples were evaluated through core flooding tests conducted on sandstone cores. According to the test results, PPG11, PPG12, and PPG13 reduced the water effluents by 22%-39%. To enhance the Water Cut Reduction (WCR), the sample with the highest WCR (PPG11) was selected, which lowered the sandstone core water effluents by 36%-39%.

Keywords-Preformed Particle Gel (PPG); SiO_2/Xanthan nanocomposites; swelling ratio; rheological study; corn oil surfactant; core flooding; Water Cut Reduction (WCR)

I. INTRODUCTION

Oil production from hydrocarbon reservoirs typically declines after years of operation [1]. To enhance recovery, water flooding is often applied; however, this technique frequently results in excessive water production through fractures and high-permeability channels connected to aquifers. Such surplus water increases the operating costs for separation and disposal, accelerates the corrosion of equipment, shortens the well life, and can ultimately lead to premature abandonment of reservoirs [2]. Therefore, there is a need for effective water shutoff technologies capable of minimizing the excess water production while maintaining or improving the hydrocarbon

recovery. Gel treatments have been widely applied to mitigate the water production by selectively plugging fractures and high-permeability zones, thereby improving the oil sweep efficiency [3]. Traditional in-situ gels, however, suffer from several limitations, including the uncontrolled gelation time, dilution by formation water, shear degradation, and the potential to damage the low-permeability zones [4].To overcome the drawbacks of PPG, a more recent version of the technology was developed, in which PPGs were synthesized using surface facilities. After drying, the gel is broken up into the appropriate sizes and injected into the desired areas [5]. The injected particles create a super-absorbent polymer capable of swelling after absorbing water, preventing or redirecting the water in the void and fracture channels in the zones of high permeability, hence reducing the water effluents and increasing the oil sweep efficiency [6].

The improvements in PPG formulations have been explored. Authors in [7] investigated NC-modified PPGs and found an improved swelling stability under high salinity. Authors in [8] reported that surfactant-assisted gels achieved higher blocking efficiency than conventional gels, while authors in [6] demonstrated that the rheological characterization of polymer gels is essential for predicting the gel propagation in porous media. Despite these advances, further evaluation is required to understand the combined effects of surfactants and NCs on swelling, viscosity, and water shutoff efficiency under simulated reservoir conditions.

The present study contributes to this field by synthesizing a novel surfactant, Sodium Methyl Ester Sulfonate (SMES), and incorporating it into PPG formulations to enhance the water shutoff performance. The PPGs were prepared using acrylamide as the polymer, N, MBA as the crosslinker, and KPS as the initiator. The effects of salinity, temperature, polymer and crosslinker concentrations, and SiO_2/xanthan NCs on the swelling behavior were systematically evaluated. A rheological assessment protocol was applied to quantify the viscosity stability under different shear rates, and sandstone core flooding experiments were performed to validate the PPG performance in reducing the water cut. These contributions provide both new materials and experimental insights that benchmark the PPG efficiency against existing literature.

II. EXPERIMENTAL DESCRIPTION

The experimental program includes the preparation of the materials and PPGs, followed by swelling tests to evaluate the absorption capacity. Next, rheological tests were conducted to determine the viscosity behavior of the samples. Finally, a core-flood test and data analysis were conducted to assess the blocking effectiveness and WCR of the synthesized PPG formulations under simulated reservoir conditions.

A. Materials

Merck (German multinational science and technology company) supplied the acrylamide, which was recrystallized from methanol and ethanol. Cross-linker MBA and initiator KPS (both from Merck) were prepared using Distilled Water, SiO_2 Nanoparticles (NPs), SiO2/Xanthan NCs, and a synthesized corn oil surfactant. NaCl, $CaCl_2$, $MgCl_2$, KCl, Na_2CO_4, and Na_2SO_4 were used without further purification. The superabsorbent polymer was also synthesized using distilled water.

1) Characterization of Green-Synthesized Nanomaterials

The mineralogical composition of the synthesized nanomaterials was investigated using Fourier-Transform Infrared Spectroscopy (FTIR) and X-ray Diffraction (XRD) to confirm the formation of ZnO NPs [9]. FTIR was employed to examine the structural features of the NPs and NCs [10], while their morphology, including size and shape, was assessed using Field Emission Scanning Electron Microscopy (FE-SEM) [11]. The thermal stability of the prepared NPs and NCs was assessed by Thermogravimetric Analysis (TGA) in the range of 25–300 °C [12]. FTIR was also used to study the interaction between SiO_2 NPs and Xanthan Gum (XG), as seen in Figure 1. The silica formation was confirmed by characteristic peaks: 471.52 cm^{-1} (Si–O–Si symmetric stretch), 643.98 cm^{-1} (SiO_4 tetrahedron vibration), and 808 cm^{-1} (Si–O bending). The 945 cm^{-1} band corresponds to Si–OH bending, while 1108.3 cm^{-1} indicates Si–O–Si asymmetric stretching. The peaks at 1418.05 cm^{-1} and 1573 cm^{-1} are attributed to COO^- stretching, whereas those at 2911 cm^{-1} and 3427 cm^{-1} represent C–H and Si–OH stretching vibrations, respectively. The disappearance of the 1734 cm^{-1} signal confirmed the silica particle formation mediated by XG.

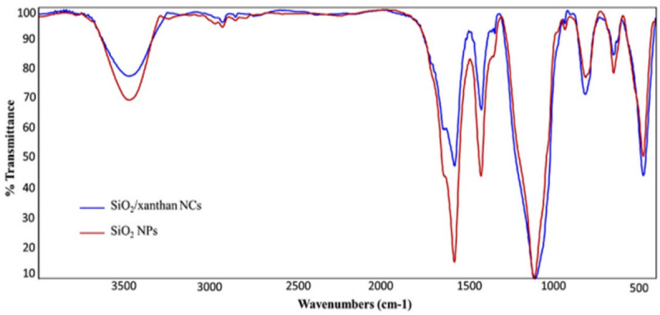

Fig. 1. The erfc-1 *P(t)/Pi* profile of the experiment as a function of root time squared.

Figure 2(a) illustrates the particle size distribution and FE-SEM micrograph of the SiO_2 NPs and SiO_2/Xanthan NCs. SiO_2 has a smooth, regular, spherical surface shape. The NPs have a diameter of 30–70 nm. The creation of larger particles is inhibited by the decreased rate of the condensation and hydrolysis reactions due to a higher concentration of OH groups in the small particles. Therefore, the powder's particle size and dispersion may be controlled by varying the amount of ethanol. Furthermore, the FE-SEM results displayed in Figure 2(b) show how the generated NCs are shaped. There are internal pores, and the surface roughness increased as a result of Xanthan's silica particle formation. The SEM data indicate that the semi-spherical, homogeneous green NCs exhibit some agglomeration. The TGA and XRD methods were used to understand the mineralogical composition of SiO_2/Xanthan NCs and SiO_2 NPs. A typical TGA spectrum and XRD pattern for nanosilica are presented in Figures 3 and 4.

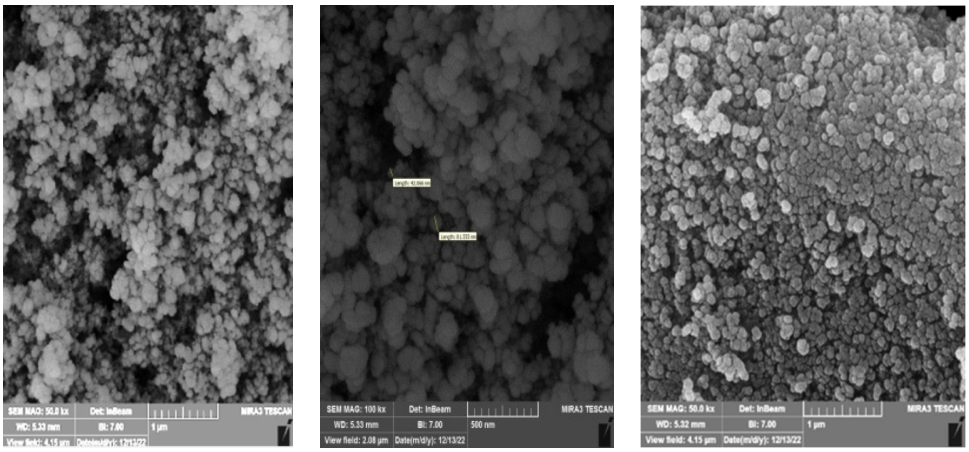

(a) (b)

Fig. 2. Size distribution of: (a)SiO2 NPs, (b) SiO2/Xanthan NCs using FE-SEM micrographs.

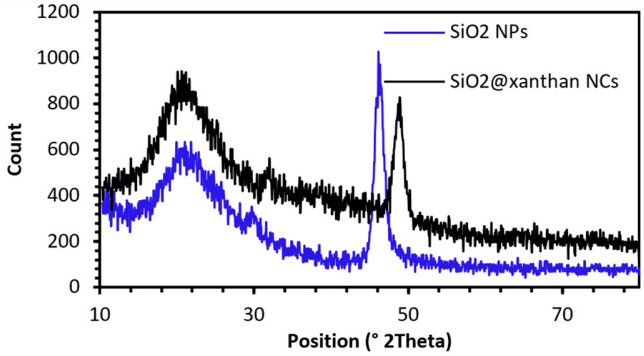

Fig. 3. XRD pattern of the SiO_2/Xanthan NCs and SiO_2 NPs.

Both Xanthan and SiO_2 NPs' crystallographic planes are represented by separate peaks in the XRD spectrum shown in Figure 3. Certain peaks exhibit how pure and crystalline certain materials are. Interestingly, the XRD pattern shows no additional diffraction peaks caused by metallic contaminants. This result indicates that the synthesized sample is free of significant metallic impurities and has a high degree of phase purity. The thermal properties of SiO_2 were investigated using TGA. Figure 4 portrays the TGA data for SiO_2 NPs and SiO_2/Xanthan NCs. It shows a weight loss peak between the starting temperatures and 170 °C, which only accounts for 20% of the overall weight loss. This implies that the SiO_2 NPs' structure remains stable at this peak. The silica nanostructures undergo a weight shift of around 60% at 300 °C, which drops to 25% at 600 °C. The third region (600 °C) accounts for most of the weight loss in the TGA study of SiO_2 NPs and SiO_2/Xanthan NCs, which is roughly 76.36% and 73.3%, respectively.

2) Synthesis and Characterization of Corn Oil Surfactant

Esterification and sulphonation were the two steps used in the production of surfactants. The oil was first mixed with 400 polyethylene glycol and 0.5% potassium hydroxide as a catalyst for esterification. To purify the ethyl ester generated in the upper layer, the resultant mixture was continuously agitated for 30 min at 70 °C before being transferred into a separating funnel. The catalyst and surplus polyethylene glycol were then filtered. The remaining fatty acids were cleaned using a solution containing sodium bicarbonate and diethyl ether. To remove the sample's moisture content, the end product of this step was evaporated for 40 min in a distillation apparatus attached to a vacuum pump.

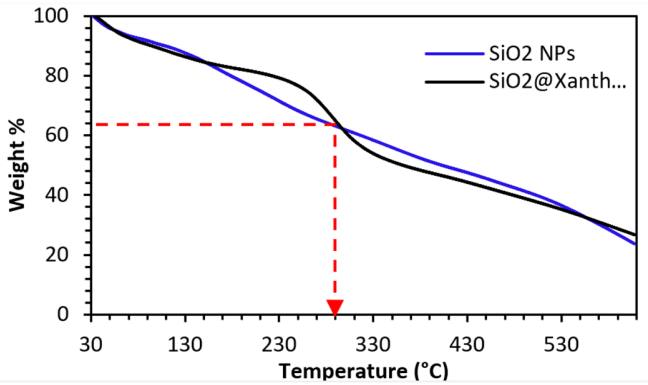

Fig. 4. Pattern of the generated SiO_2 NPs and SiO_2/Xanthan NCs using TGA.

At this point, a creamy, thick liquid was produced. To create a clear solution, 5.40 g of chlorosulphonic acid and 30 ml of pyridine were added to a round-bottom flask and swirled for 30 min at 60 °C. Sodium carbonate and sodium bicarbonate saturation solutions were used in a separating funnel to quench the solution. Nonreactive organic debris was removed using a 50 ml solution of n-butanol. Water and pyridine were separated by evaporating the aqueous layer containing the finished product at 120 °C. The final sodium ethyl ester sulfonate anionic surfactant was obtained as a white powder after the product was evaporated for 40 min in a distillation apparatus connected to a vacuum pump.

a) Fourier-Transform Infrared Spectroscopy

A small amount of surfactant combined with KBr was utilized to determine the functional groups of the natural surfactant that was isolated from the corn seed using FTIR analysis, as depicted in Figure 5. The Tensor 27 FT-IR Bruker spectroscopy was used to record the infrared spectra. With its

370–7500 cm^{-1} spectrum and MIR-acle-attenuated total reflectance accessory, the spectroscopy aids in the analysis of both the liquid and solid materials. The S-O stretching vibrations are associated with the peaks at 623 and 861 cm^{-1}. The S=O bond in the sulfonate group is visible at the peak at 1112 cm^{-1}. The sulfonation process is connected to these peaks.

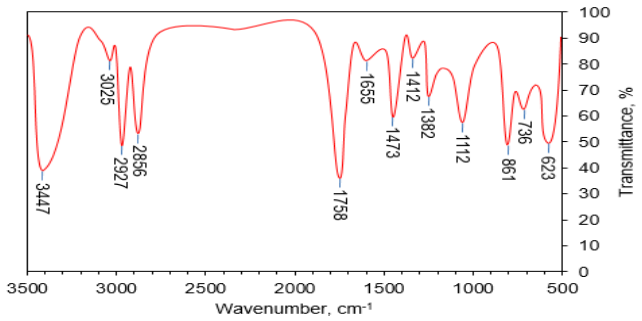

Fig. 5. FTIR analysis of corn oil surfactant.

b) Thermogravimetric Analysis

A Netzsch TG209 F1 analyzer was used to perform TGA on 15 mg of the surfactant sample. The analysis was conducted in a pure nitrogen environment. The sample was heated from 20 to 300 °C at a rate of 10 °C/min with a flow rate of 30 mL/min. The purpose of this analysis was to verify the synthetic surfactant's thermal stability. An 11% weight loss was observed at 112 °C due to sample moisture (hydration). The weight change reached 59% at 300 °C, indicating molecular restructuring. These TGA results show that the synthesized natural surfactant derived from corn seed is suitable for high-temperature oil reservoirs. The temperature stability is inherent to the surfactant itself and not to the surfactant solution, which would yield different TGA results.

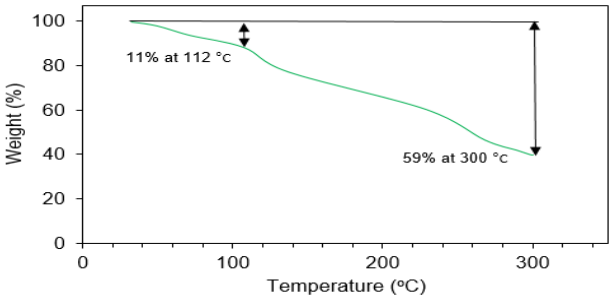

Fig. 6. TGA analysis of corn oil surfactant.

B. Preformed Particle Gel Preparation

Initially, a homogeneous solution was prepared by dissolving acrylamide powder in distilled water. After 10 min of thorough mixing with a magnetic stirrer, the resulting polymer solution reacted with the crosslinker MBA and the initiator, KPS, to form a gellant solution. Subsequently, SiO_2/Xanthan NCs and corn oil surfactant (sodium ethyl ester sulfonate, an anionic surfactant) were added to enhance the PPG properties. The gellant was then transferred into sealed tubes and stored in an oven at 30 °C for 48 h. After the formation of the 3D gellant structure, the samples were placed again in an oven at 30 °C for 24 h to obtain completely dried polymer gels. Finally, the dried gels were broken into pieces to obtain the desired PPGs.

TABLE I. PPG SAMPLES AND MATERIALS USED (IN ppm).

Sample	AAM (ppm)	MBA (ppm)	KPS (ppm)	Corn oil surfactant (ppm)	SiO_2/ Xanthan NCs (ppm)	Distilled water (ppm)
PPG 1	20000	2000	20	0	0	977980
PPG 2	20000	4000	40	0	0	975960
PPG 3	20000	6000	60	0	0	973940
PPG 4	30000	2000	20	0	0	967980
PPG 5	30000	4000	40	0	0	965960
PPG 6	30000	6000	60	0	0	963940
PPG 7	40000	2000	20	0	0	957980
PPG 8	40000	4000	40	0	0	955960
PPG 9	40000	6000	60	0	0	953940
PPG 10	20000	2000	20	0	1000	976980
PPG 11	20000	2000	20	500	1000	976480
PPG 12	20000	2000	20	1000	1000	975980
PPG 13	20000	2000	20	1500	1000	975480

C. Measurement of Swelling Ratio

The gravimetric approach was used to measure the PPG's water absorption or swelling ratio. 400 mm of water were used to soak a known weight of dry PPG for 1 h. After this period, a paper filter was used to separate the remaining water in the container from the swollen PPG. The swelling ratio of the swollen PPG was calculated using (1), as presented in [13]. The weight balance measurement uncertainty was ±0.1 mg.

$$SR = \frac{m_{swollen} - m_{dry}}{m_{dry}} \quad (1)$$

where $m_{swollen}$ and m_{dry} represent the dry and swollen weights of the PPG, respectively.

D. Rheological Investigations

The rheological properties of the prepared PPG were analyzed using an MCR502 Rheometer (Anton Paar Co.). A parallel plate setup was employed, featuring 50 mm in diameter plates, with a 3 mm plate spacing. To ensure

consistent testing conditions, the samples were uniformly shaped, each measuring 2 cm in diameter and 2 mm in height. Measurements were conducted at 60, 100, and 120 rpm. The measurement uncertainty and error were ±0.05 Pa·s.

E. Test of Experimental Work

Figure 7 illustrates the core flooding unit. The equipment consists of three transfer containers, a syringe pump, a hand pump, a core holder, and a pressure transducer that records the pressure readings via connection to a computer. Using the hand pump, a rubber sleeve is inserted within the core holder to seal the space around the sand pack and prevent leaks. Sand particles are gradually added within the rubber sleeve and evenly packed under continuous pressure to ensure uniform porosity throughout the sand pack. The measurement uncertainty and error were ±0.2 mL/min.

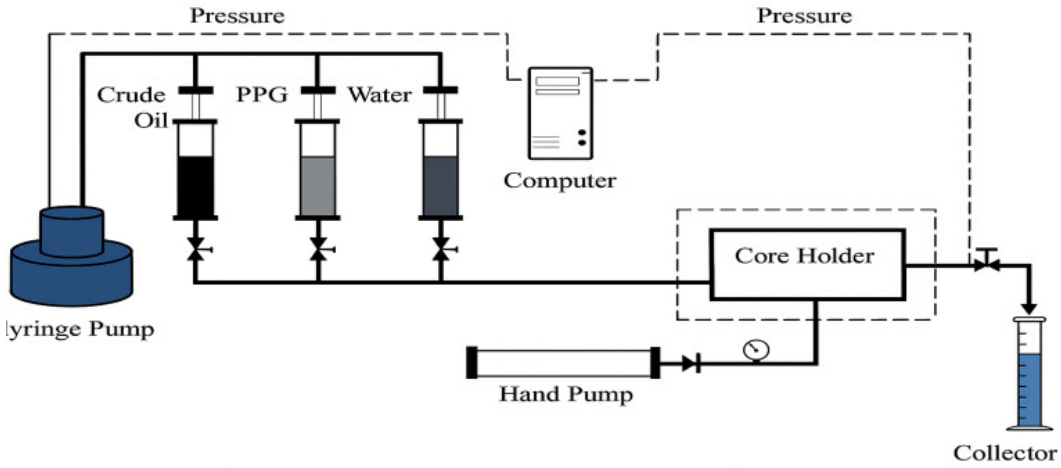

Fig. 7. Schematic representation of the core flooding experimental setup.

1) The Process of Core Flooding

The core flooding test was deployed to assess the PPG's effectiveness in reducing the water production in the core of sandstone using the following steps:

- The porosity of the core was assessed after it had been saturated with formation water.
- The Darcy equation was used to calculate the absolute permeability of the core after formation water was introduced at various flow rates.
- Crude oil was pumped into the core to displace the water until the core reached its residual water saturation.
- Formation water was injected into the core under various constant pressures, and the water effluent from each test was collected in a single container.
- The swollen PPG was injected into the core.
- After PPG injection, formation water was again injected at different constant pressures, and the effluent from each test was collected in a container.
- For each applied pressure, the WCR% in the core due to PPG was calculated using the relation given in [14]:

$$WCR\% = \frac{Q_{Before} - Q_{After}}{Q_{Before}} \times 100 \quad (2)$$

where Q_{Before} and Q_{after} represent the effluent water from the core of sandstone before and after the PPG injection, respectively.

III. RESULTS AND DISCUSSION

A. Swelling Ratio of the Gel

1) The Impact of Initiator, Cross-Linker, and Polymer Concentrations on the PPG Swelling Ratio

To investigate the effect of the polymer and cross-linker concentrations on the PPG swelling ratio, nine samples with various polymer concentrations of 20,000, 30,000, and 40,000 ppm, and cross-linker with initiator combinations of 2,000–20, 4,000–40, and 6,000–60 ppm were prepared. The swelling ratio of each sample was determined after soaking in distilled water at room temperature for 1 h. A PPG sample is shown in Figure 8, both before and after soaking in distilled water. Figure 9 demonstrates that the PPG swollen in distilled water, with a volume equal to 100 times the dry PPG volume, exhibited a significant increase in the PPG volume ratio.

The effect of polymer and (cross-linker and initiator) concentrations on the swelling ratio of PPG is shown in Figure 9. At 20,000 ppm, the swelling ratio is 250 grams of water absorbed per gram of dry gel (g/g). It is evident that the PPG sample soaked in distilled water for 1 h has a swelling ratio 100 units higher than its dry equivalent. Increasing the concentrations of polymer and (cross-linker and initiator) leads to the formation of excessively thick three-dimensional network structures with very small pore sizes. As a result, large volumes of water cannot penetrate the 3D polymer gel network because the rigid and dense structure acts as a steric barrier to hydrogel expansion. Consequently, the water-holding capacity of PPG decreases as the concentrations of polymer and (cross-linker and initiator) increase.

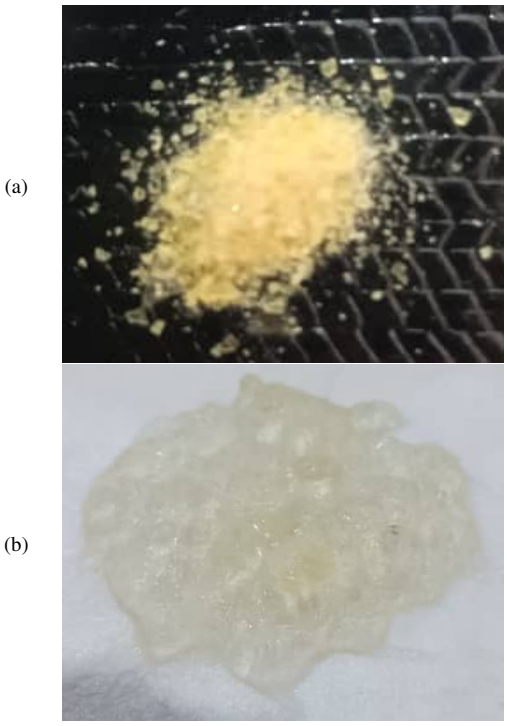

Fig. 8. PPG: (a) before swelling, (b) after swelling in distilled water.

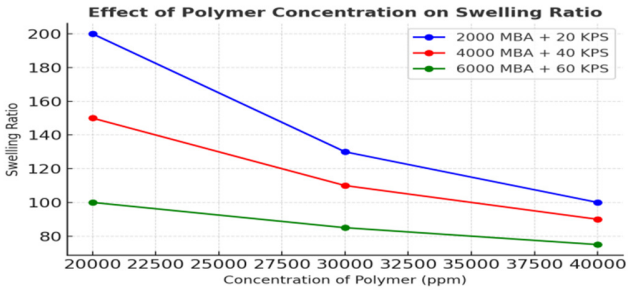

Fig. 9. Effect of polymer and (cross-linker and initiator) concentrations on the swelling ratio of PPG.

2) *Effect of Salinity on the PPG Swelling Ratio*

Figure 10 illustrates the effect of KCl on the swelling behavior of PPG. When KCl is introduced, it increases the ionic strength of the surrounding solution. At salinity levels above 25,000 ppm, the swelling ratio approaches zero, whereas at 0 ppm, the swelling ratio reaches its maximum, which is 250 g/g. The presence of KCl reduces the osmotic pressure difference, lowering the driving force for the water absorption and, thereby, limiting the gel swelling. Additionally, K^+ ions shield the negatively charged groups formed during KPS decomposition. Without ionic shielding, these negative charges repel each other, keeping the gel expanded. However, in the presence of KCl, this repulsion decreases, allowing polymer chains to move closer, compacting the gel structure. As a result, the gel becomes denser and less capable of absorbing water. The effect intensifies with an increasing KCl concentration. At low concentrations (e.g., 0.1%), moderate swelling is still observed, but at higher levels (e.g., 1% or more), the swelling ratio decreases sharply. Although KCl, a monovalent salt, has a weaker impact than that of divalent salts such as $CaCl_2$, it still plays a significant role in regulating the swelling behavior and mechanical properties of acrylamide-based gels.

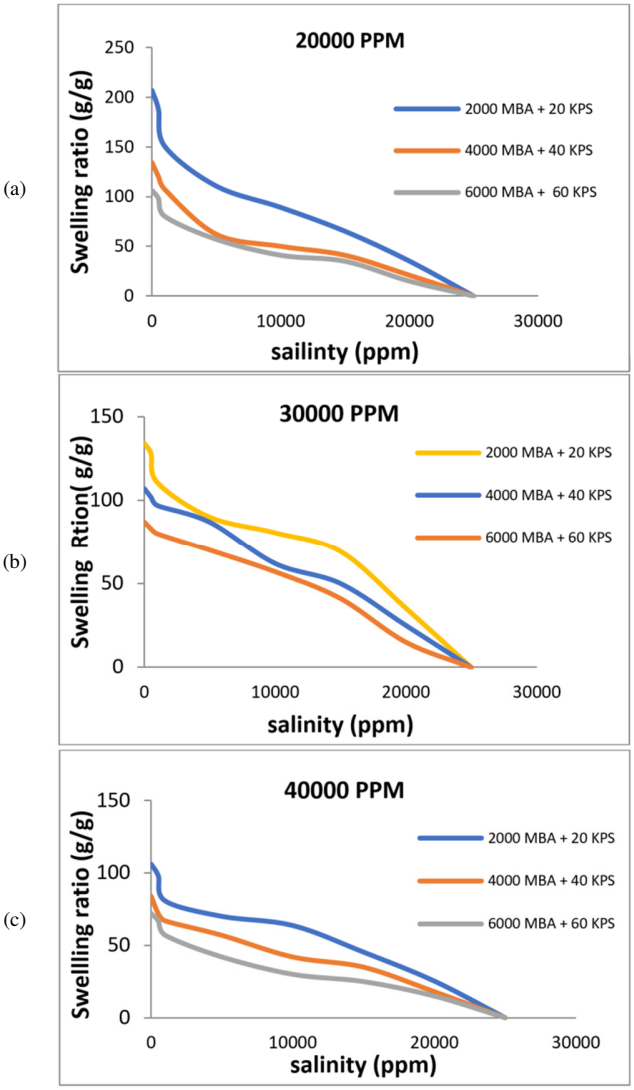

Fig. 10. Impact of salinity on the PPG swelling ratio for polymer concentrations of: (a) 20,000 ppm, (b) 30,000 ppm, and (c) 40,000 ppm.

3) *Effect of SiO_2/Xanthan NCs on the PPG Swelling Ratio*

In Figure 11, based on the high swelling ratio value, when acrylamide is fixed at 20,000 ppm and the crosslinker MBA and the initiator KOS, the addition of 1,000 ppm of SiO_2/Xanthan NCs significantly changed the wettability of the utilized carbonate rock from a strong oil-wet to a strong water-wet system, decreasing the contact angle from 134° to 28° by adding 1,000 ppm of the synthesized NC to distilled water [15], which leads to a significant decrease in the swelling ratio; that is, to 90 g/g when the PPG1 is used, approximately 50% lower compared to the same formulations without the NCs. This reduction is attributed to the dual role of the NCs in the hydrogel network. While SiO_2 and Xanthan are generally

hydrophilic and known to enhance swelling under certain conditions.

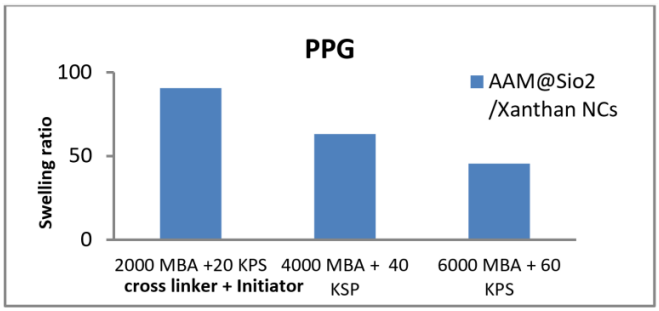

Fig. 11. Effect of 1000 ppm of SiO_2/Xanthan NCs on the PPG swelling ratio for polymer concentrations of 20,000 ppm.

The incorporation of SiO_2/Xanthan NCs into acrylamide-based hydrogels provides significant improvements in the mechanical, thermal, and functional properties. A key advantage is the reinforcement of the polymer network: SiO_2 NPs add inorganic strength, enhancing the resistance to deformation and improving the stability under stress or temperature variations. At the same time, XG, a natural polysaccharide, increases the hydrophilicity of the gel, promoting a higher water retention and, under optimized conditions, a greater swelling ratio. The NCs also modify the porosity and internal structure of the hydrogel, which is valuable for applications such as drug delivery, water shut-off treatments in petroleum reservoirs, and controlled release systems. Furthermore, functional groups introduced by SiO_2/Xanthan NCs, such as hydroxyl and carboxyl, can interact with surrounding ions or molecules, enabling the responsiveness to external stimuli, like pH or salinity changes. However, excessive NC loading or high crosslinking density may create a dense network that restricts swelling. Therefore, the optimization of the NC concentration is essential. Overall, SiO_2/Xanthan NCs enhance the hydrogel strength, responsiveness, and adaptability for advanced applications.

B. Rheological Studies

The Samples of PPG 1, PPG 4, and PPG 6, containing polymer concentrations of 20000, 30,000, and 40,000 ppm, respectively, were chosen for the frequency sweep test to evaluate the viscosity of the PPGs, while maintaining a constant crosslinker and initiator concentration of 2000 and 20 ppm. After that, 1000 ppm of SiO_2/Xanthan NCs was added. All samples used distilled water during preparation for the rheological measurements. Figure 12 illustrates how the concentration of polymer and viscosity moduli of the three samples change with frequency.

At 20000 ppm of acrylamide at a constant crosslinker and initiator concentration of 2000 ppm and 20 ppm with 1000 ppm of SiO_2/Xanthan NCs, the viscosity remained the same at 2.5 cP at different stirring rates (60 rpm, 100 rpm, 120 rpm). The PPG 10 sample can then be used with corn oil surfactant (sodium ethyl ester sulfonate anionic surfactant) in polymer and gel systems due to its ability to stabilize the emulsions and improve the dispersion of hydrophobic or poorly soluble components, such as nanoparticles or organic additives. It functions as a natural, biodegradable surfactant that reduces the surface tension between different phases, resulting in a more uniform and homogeneous mixture. In formulations involving NPs, like SiO_2 or natural polymers such as XG, the corn oil surfactant helps to evenly distribute these components throughout the gel matrix, preventing aggregation and enhancing the overall consistency and mechanical strength of the gel. Furthermore, it improves the interfacial interaction between the hydrophilic and hydrophobic regions in the system, contributing to a better gel stability and more controlled swelling behavior. Given that corn oil is plant-based and non-toxic, it supports environmentally friendly and sustainable formulations. However, its concentration must be carefully optimized, as excessive amounts can interfere with the polymerization process or weaken the final gel structure.

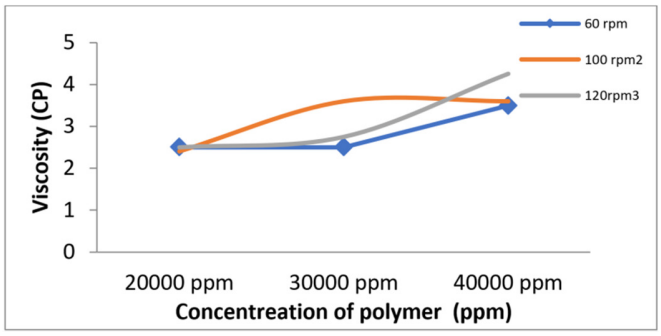

Fig. 12. Variations in the viscosity and concentration of polymer at constant crosslinker and initiator concentration of 2000 and 20 ppm with 1000 PPM of SiO_2/Xanthan NCs.

Figure 13 shows that the viscosity remained stable at 20,000 ppm, suggesting the formation of a three-dimensional network structure in all three swollen PPG samples. The higher viscosity values indicate that the samples exhibited a more elastic than viscous behavior. Notably, PPG 11, 12, and 13, which contained polymer with corn oil surfactant, demonstrated a greater viscosity and, therefore, a stronger structural integrity. This enhanced the viscosity, and allowed them to better resist the pressure drops and shear forces during the PPG injection and diffusion in the reservoir. Some highly viscous samples also showed the ability to deform under stress and recover their original shape once the stress was removed.

With increasing concentrations of SiO_2/Xanthan NCs and corn oil surfactant, the rheological properties of the gels further improved. Samples 11, 12, and 13, in particular, exhibited higher elastic moduli and stronger structural stability, enabling superior resistance to mechanical stresses. Although higher concentrations of polymer, SiO_2/Xanthan NCs, and surfactant reduced the swelling ratio, they significantly decreased the sensitivity to salinity by reinforcing the gel network. These improved viscoelastic properties make the modified hydrogel more effective for core flooding applications. This study highlights the role of SiO_2/Xanthan NCs and corn oil surfactant in enhancing both the swelling and rheological performance of acrylamide-based systems.

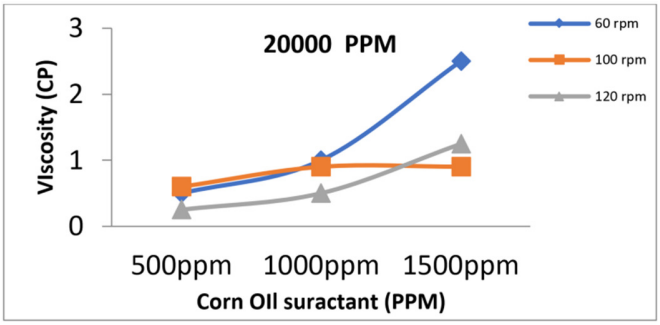

Fig. 13. Variations in the viscosity and concentration of polymer at constant crosslinker and initiator concentration of 2000 and 20 ppm with 1000 ppm of SiO_2/Xanthan NCs.

C. Water Shut-Off Technique

The core flooding test was conducted under constant pressure to evaluate the effectiveness of PPG 11, 12, and 13 in reducing the water cut within sandstone. Three previously characterized plugs treated with PPG 11, 12, and 13, selected based on their rheological properties and swelling ratios, were used in this analysis. The properties of the prepared plugs and PPG samples are summarized in Table II. Table III presents formation water effluent data before and after the PPG injection. The results show a clear decline in the water output from the sandstone, attributed to the PPG particles plugging pore spaces and blocking the water pathways. Their elastic nature allowed the particles to deform and adapt to the pore structure, reducing the sandstone permeability and further lowering the water production [16]. Equation (2) was used to calculate the percentage of WCR in formation water for the three sandstone plugs, as illustrated in Figure 14. The PPGs formulated with polyacrylamide, SiO_2/Xanthan NCs, and corn oil surfactant reduced the water production by approximately 22–39%. The highest reduction (36–39%) was observed in Plug 1, which received PPG 11 formulated with 20,000 ppm polymer, 2,000 ppm crosslinker, 20 ppm initiator, 1,000 ppm SiO_2/Xanthan NCs, and 1,500 ppm corn oil surfactant. As noted in the rheological analysis, the high polymer concentration in this sample produced stronger gel particles, offering greater resistance to formation water flow, reducing the water output.

All three plugs exhibited a gradual decline in the water cut. The PPGs experienced partial dehydration upon contact with salts, reducing the particle volume and contributing to performance loss. In addition, some particles were flushed out under injection pressure, which diminished efficiency. However, once the PPGs sufficiently occupied pore spaces, further WCR became minimal.

TABLE II. PROPERTIES OF PPG SAMPLES AND SAND PACKS USED IN CORE FLOODING EXPERIMENTS (SANDSTONE)

Property	Plug 1	Plug 2	Plug 3
PPG	11	12	13
Length, cm	8.5	8.5	8.5
Diameter, cm	3.81	3.81	3.81
Porosity, %	22.59	21.08	21.54
Permeability, mD	489.76	473.05	478.19
Pore Volume, ml	21.88	20.42	20.85

TABLE III. WCR BEFORE AND AFTER PPG INJECTION AT VARIOUS PRESSURE GRADIENTS

ΔP (psi)	Plug 1 Before	Plug 1 After	Plug 2 Before	Plug 2 After	Plug 3 Before	Plug 3 After
39.51	68.00	41.00	63.00	49.00	65.00	43.00
41.36	71.00	45.00	64.00	47.00	72.00	46.00
43.19	73.00	46.00	67.00	44.00	69.00	44.00

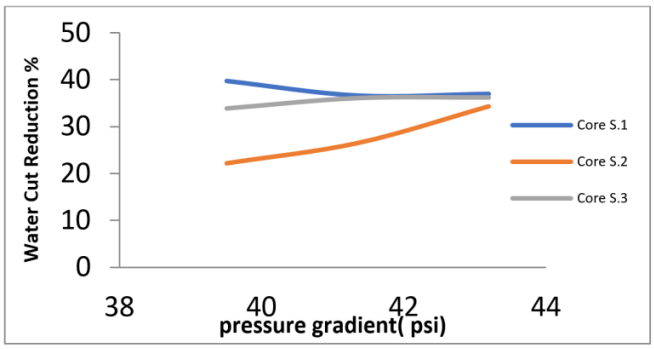

Fig. 14. PPG's WCR versus pressure gradient.

IV. CONCLUSIONS

This study investigated the effectiveness of Preformed Particle Gels (PPGs) synthesized from acrylamide, N, N-methylenebisacrylamide (MBA), Potassium Persulfate (KPS), SiO_2/xanthan Nanocomposites (NCs), and a corn-oil-derived surfactant for water shutoff applications in sandstone reservoirs. The PPGs exhibited a superabsorbent behavior, with swelling ratios up to 250 grams of water absorbed per gram of dry gel (g/g) in distilled water. The swelling performance decreased under higher salinity conditions due to the ionic effects of dissolved salts. Among the formulations, the gels containing 20,000 ppm polymer, 2,000 ppm crosslinker, and 20 ppm initiator demonstrated the lowest salt sensitivity, indicating an optimal balance between the gel strength and swelling capacity. Incorporating 1,000 ppm SiO_2/xanthan NCs reduced the swelling ratio, highlighting the need for careful optimization of the NC content. In contrast, the addition of surfactant at concentrations of 500–1,500 ppm enhanced the viscosity stability, and pore-filling efficiency, maintaining the gel performance under shear conditions. The core flooding experiments confirmed that the surfactant-modified PPG11 (500 ppm surfactant) achieved the highest Water Cut Reduction (WCR), ranging from 36% to 39%. These results demonstrate that surfactant-reinforced PPGs can effectively control the water production and improve the oil sweep efficiency in sandstone reservoirs. Although some dehydration occurs upon prolonged contact with formation water, PPG11 is proposed for field application due to its superior swelling stability, rheological performance, and water shutoff effectiveness. Future studies should explore the long-term stability, optimize the NC concentrations, and conduct pilot-scale trials to validate performance under simulated reservoir conditions.

ACKNOWLEDGEMENT

The authors would like to express their sincere gratitude to the Department of Petroleum Engineering and the Department

of Chemistry Science at the University of Zakho for their support and sponsorship of this research. They also extend their appreciation to all individuals who contributed to and assisted in the completion of this work.

REFERENCES

[1] M. O. Elsharafi and B. Bai, "Effect of Weak Preformed Particle Gel on Unswept Oil Zones/Areas during Conformance Control Treatments," *Industrial & Engineering Chemistry Research*, vol. 51, no. 35, pp. 11547–11554, Sept. 2012, https://doi.org/10.1021/ie3007227.

[2] M. Abedi Lenji, M. Haghshenasfard, M. Vafaie Sefti, M. Baghban Salehi, and A. Mousavi Moghadam, "Numerical Modeling and Experimental Investigation of Inorganic and Organic Crosslinkers Effects on Polymer Gel Properties," *Journal of Petroleum Science and Engineering*, vol. 160, pp. 160–169, Jan. 2018, https://doi.org/10.1016/j.petrol.2017.10.045.

[3] A. Goudarzi *et al.*, "A Laboratory and Simulation Study of Preformed Particle Gels for Water Conformance Control," *Fuel*, vol. 140, pp. 502–513, Jan. 2015, https://doi.org/10.1016/j.fuel.2014.09.081.

[4] G. Zhao *et al.*, "Preparation and Application of a Novel Phenolic Resin Dispersed Particle Gel for in-Depth Profile Control in Low Permeability Reservoirs," *Journal of Petroleum Science and Engineering*, vol. 161, pp. 703–714, Feb. 2018, https://doi.org/10.1016/j.petrol.2017.11.070.

[5] H. R. Saghafi, M. A. Emadi, A. Farasat, M. Arabloo, and A. Naderifar, "Performance Evaluation of Optimized Preformed Particle Gel (PPG) in Porous Media," *Chemical Engineering Research and Design*, vol. 112, pp. 175–189, Aug. 2016, https://doi.org/10.1016/j.cherd.2016.06.004.

[6] A. Farasat, M. Vafaie Sefti, S. Sadeghnejad, and H. R. Saghafi, "Mechanical Entrapment Analysis of Enhanced Preformed Particle Gels (PPGs) in Mature Reservoirs," *Journal of Petroleum Science and Engineering*, vol. 157, pp. 441–450, Aug. 2017, https://doi.org/10.1016/j.petrol.2017.07.028.

[7] P. Tongwa and B. Bai, "Degradable Nanocomposite Preformed Particle Gel for Chemical Enhanced Oil Recovery Applications," *Journal of Petroleum Science and Engineering*, vol. 124, pp. 35–45, Dec. 2014, https://doi.org/10.1016/j.petrol.2014.10.011.

[8] X. Chen, Q. Feng, W. Liu, and K. Sepehrnoori, "Modeling Preformed Particle Gel Surfactant Combined Flooding for Enhanced Oil Recovery After Polymer Flooding," *Fuel*, vol. 194, pp. 42–49, Apr. 2017, https://doi.org/10.1016/j.fuel.2016.12.075.

[9] A. Mir, N. Becheikh, L. Khezami, M. Bououdina, and A. Ouderni, "Synthesis, Characterization, and Study of the Photocatalytic Activity upon Polymeric-Surface Modification of ZnO Nanoparticles," *Engineering, Technology & Applied Science Research*, vol. 13, no. 6, pp. 12047–12053, Dec. 2023, https://doi.org/10.48084/etasr.6373.

[10] M. Njjar, E. Z. Aktürk, A. Kaya, C. Onac, and A. Akdogan, "A Novel MIP Electrochemical Sensor Based on a $CuFe_2$ O_4 NPs@rGO Nanocomposite and its Application in Breast Milk Samples for the Determination of Fipronil," *Analytical Methods*, vol. 17, no. 26, pp. 5508–5518, 2025, https://doi.org/10.1039/D5AY00911A.

[11] D. A. Kadhim, M. A. Abid, and W. M. Salih, "Photocatalytic Activity for Degradation of Methylene Blue Dye-Mediated Nanocomposite-Copper Oxide/Graphene Oxide Preparation from Blood Solution via Hydrothermal Method with Laser Irradiation," *Vacuum*, vol. 228, Oct. 2024, Art. no. 113481, https://doi.org/10.1016/j.vacuum.2024.113481.

[12] G. B. Vaggar, "An Investigation of Thermogravimetric Analysis and Thermal Conductivity of Glass Fibre Epoxy Resin Composites Modified with Silicon Carbide, Manganese, and Copper Nanoparticles (NPs)," in *the Materials Joining and Manufacturing Processes*, 2025, pp. 57–63, https://doi.org/10.21741/9781644903612-10.

[13] S. Suresh, "Evaluation of Swelling and Re-Swelling of Preformed Particle Gels (PPG) When Exposed to CO2," M.S. thesis, Missouri University of Science and Technology, Rolla, MO, USA, 2017.

[14] H. Zhang and B. Bai, "Preformed-Particle-Gel Transport Through Open Fractures and Its Effect on Water Flow," *SPE Journal*, vol. 16, no. 02, pp. 388–400, June 2011, https://doi.org/10.2118/129908-PA.

[15] J. Ali, A. K. Manshad, I. Imani, S. M. Sajadi, and A. Keshavarz, "Greenly Synthesized Magnetite@SiO2@Xanthan Nanocomposites and Its Application in Enhanced Oil Recovery: IFT Reduction and Wettability Alteration," *Arabian Journal for Science and Engineering*, vol. 45, no. 9, pp. 7751–7761, Sept. 2020, https://doi.org/10.1007/s13369-020-04377-x.

[16] Q. Sang, Y. Li, L. Yu, Z. Li, and M. Dong, "Enhanced Oil Recovery by Branched-preformed Particle Gel Injection in Parallel-sandpack Models," *Fuel*, vol. 136, pp. 295–306, Nov. 2014, https://doi.org/10.1016/j.fuel.2014.07.065.